

extent of dissociation if the reaction were in equilibrium at the local conditions, k is the dissociation reaction rate "constant," M_2 is the molecular weight of the dimer, and ΔH is the heat of dissociation of the dimer. Other symbols are standard.

Recognizing, from (5), that

$$\frac{dx}{du} = \frac{d \ln A}{du} \frac{1}{F(x)} \quad (7)$$

we can get an expression for the rate of reaction:

$$\frac{d\alpha}{du} = \frac{k\Delta}{uF} \frac{d \ln A}{du} \quad (8)$$

Solving (4) for $(1/\rho)(d\rho/du)$, substituting into it (2, 3, and 8), recognizing that $\gamma M_f^2 = \rho(u^2/P)$, $u^2 M_2/TC_p = (\gamma - 1)M_f^2$, where γ is the ratio of specific heats, and letting $m = \Delta H/RT$, $g' = C_p/R$, and $\Gamma = \{[(1 + \alpha)m]/g'\} - 1$, we obtain

$$\frac{1}{\rho} \frac{d\rho}{du} = -\frac{M_f^2}{u} + \frac{\Gamma}{1 + \alpha} \frac{k\Delta}{uF} \frac{d \ln A}{du} \quad (9)$$

We can now eliminate $(1/\rho)(d\rho/du)$ using (1) and can arrive at an expression for†

$$\frac{d \ln A}{du} = \frac{M_f^2 - 1}{u} \left\{ 1 + \frac{\Gamma k\Delta}{(1 + \alpha)uF} \right\}^{-1} \quad (10)$$

Let us define $\psi = \Gamma k\Delta/[(1 + \alpha)uF]$. We can now substitute (10) into (8), obtaining a rate equation of the form

$$\frac{d\alpha}{du} = \frac{(M_f^2 - 1)}{u} \frac{\psi(1 + \alpha)}{\Gamma(1 + \psi)} \quad (11)$$

Using this equation and (3), we can get an expression for $d \ln T/d \ln u$

$$d \ln T/d \ln u = -[(\gamma + \phi - 1)M_f^2 - \phi] \quad (12)$$

where $\phi = \psi(\Gamma + 1)/\Gamma(\psi + 1)$

One criterion of stability is that $d \ln T/d \ln u < 0$. Hence from (12), $(\gamma - 1 + \phi)M_f^2 - \phi > 0$. Solving for ϕ , ψ , and finally Δ , we get

$$\phi < [(\gamma - 1)M_f^2]/(1 - M_f^2) \quad (13)$$

$$\psi < \frac{[\Gamma/(\Gamma + 1)](\gamma - 1)}{[(1 - M_f^2)/M_f^2] - [\Gamma/(\Gamma + 1)](\gamma - 1)} \quad (14)$$

and

$$\Delta < \frac{(1 + \alpha)uF}{k} \left\{ \frac{[\Gamma/(\Gamma + 1)](\gamma - 1)}{[(1 - M_f^2)/M_f^2] - [\Gamma/(\Gamma + 1)](\gamma - 1)} \right\} \quad (15)$$

Note that Δ represents a measure of the deviation from equilibrium [see Eq. (6)]. We can rewrite (15) as follows:

$$\Delta < \frac{\mu(1 + \alpha)F(x')}{D} \times \left\{ \frac{[\Gamma/(\Gamma + 1)](\gamma - 1)}{[(1 - M_f^2)/M_f^2] - [\Gamma/(\Gamma + 1)](\gamma - 1)} \right\} \quad (16)$$

where $\mu = u/a$, $F(x') = d \ln A/dx'$, $D = lk/a$, $x' = x/l$, l is some characteristic length, and $a = P_0/\rho_0$ is Newton's velocity of sound at chamber conditions.

As a numerical example, let $\mu = 0.04$, $M_f = 0.04$, $F(x') = -100$, $D = 1000$, $\alpha = 0.2$, $\Gamma = 4$, and $\gamma = 1.2$. For stability, $\phi < 4.01 \times 10^{-7}$, $\psi < 3.57 \times 10^{-3}$, and $\Delta < -4.29 \times 10^{-7}$.

† Note that the singularity in the equations has been shifted to the point where $\psi = -1$. This point occurs in the supersonic region.

It is obvious that stability of the nonequilibrium hodograph equations in the subsonic region is achieved only if the gas is extremely near equilibrium. Note that these equations appear more stable the closer one gets to equilibrium, apparently behaving in a manner opposite to the physical equations.⁴ In general, however, the hodograph equations are not stable for most regions of interest.

This stability criterion can also be applied to equilibrium and frozen flows with predicted results. For equilibrium flow, it can be shown that⁵

$$\frac{d\alpha}{du} = \frac{\beta m}{T} \frac{dT}{du} - \frac{\beta}{P} \frac{dP}{du} \quad (17)$$

where $\beta = [\alpha(1 - \alpha^2)]/2$. Using this equation, along with (2) and (3), one can arrive at an equation similar to (12):

$$\frac{d \ln T}{d \ln u} = -\frac{(\gamma^e - 1)M_e^2\{1 + [\beta m/(1 + \alpha)]\}}{[1 + (\beta m/g')]} \quad (18)$$

where M_e is now the Mach number based on the equilibrium velocity of sound, and γ^e is defined as $\gamma^e = a^2 P/\rho$, where a_e is the equilibrium velocity of sound.³ Since $\alpha, \beta, m, \gamma^e, g' > 0$ for an exothermic recombination reaction and $\gamma^e > 1$, $d \ln T/d \ln u$ is always less than zero. Hence the equilibrium equations are stable everywhere.

For the frozen hodograph equations, by setting $d\alpha/du = 0$, we can show that

$$d \ln T/d \ln u = -(\gamma - 1)M_f^2 \quad (19)$$

and again $d \ln T/d \ln u < 0$ everywhere, meaning that the frozen hodograph equations are also stable everywhere.

There is little reason to believe that this stability criterion is the best, but it qualitatively agrees with the author's computing experience on these equations.

References

- ¹ Sarli, V. J., Blackman, A. W., and Buswell, R. F., "Kinetic of hydrogen-air flow systems. II. Calculations of nozzle flows for ramjets," *Ninth Symposium (International) on Combustion* (Academic Press, Inc., New York, 1962), p. 572.
- ² Westenberg, A. A., and Favin, S., "Nozzle flow with complex chemical reaction," Johns Hopkins Univ., Appl. Phys. Lab. Rept. CM-1013, Silver Spring, Md., p. 13 (March 1962).
- ³ Throne, J. L., "One dimensional isentropic reacting gas flow in a nozzle," MS Ch E Thesis, Univ. Delaware, Newark, Del., p. 36 (June 1961).
- ⁴ Emanuel, G., "Problems underlying the numerical integration of the chemical and vibrational rate equations in a near-equilibrium flow," Arnold Eng. Dev. Center AEDC-TDR-63-82, Dept. Aeronaut. Astronaut., Stanford Univ., Stanford, Calif., p. 15 (March 1963).

Flow in the Three-Dimensional Boundary Layer on a Spinning Body of Revolution

O. PARR*

Institute of Fluid Mechanics of the Technical University, Braunschweig, Germany

THE flow on a body of revolution spinning about its axis, which is parallel to a stream, is of some practical importance. The flow on a spinning projectile and on the hub of an axial turbomachine are typical examples. The problem has been dealt with experimentally by Wieselsberger¹

Received September 12, 1963

* Research Collaborator

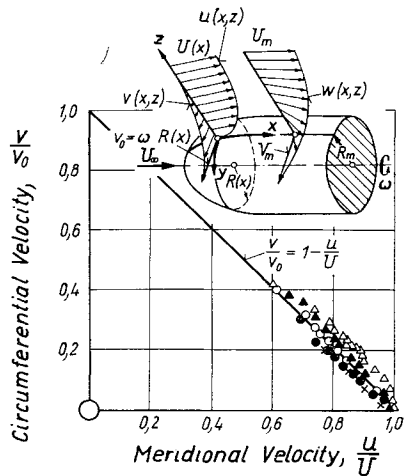


Fig 1 Velocity distribution in the turbulent boundary layer on a rotating body of revolution in axial flow; $Re_m = 3 \times 10^5$

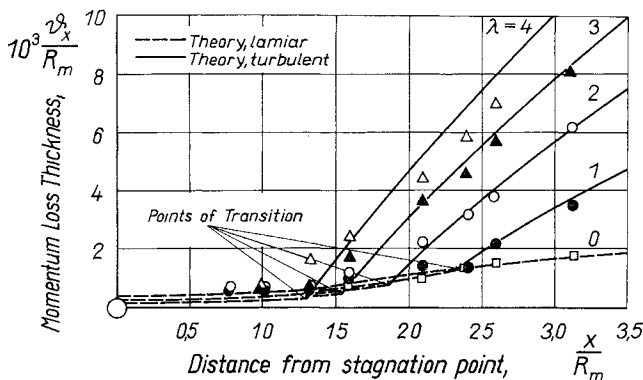


Fig 2 Meridional momentum loss thickness ϑ_x as defined by Eq (2) on a spinning body of revolution; theory and experiment, $Re_m = 3 \times 10^5$, $\lambda = R_m \omega / U_m$

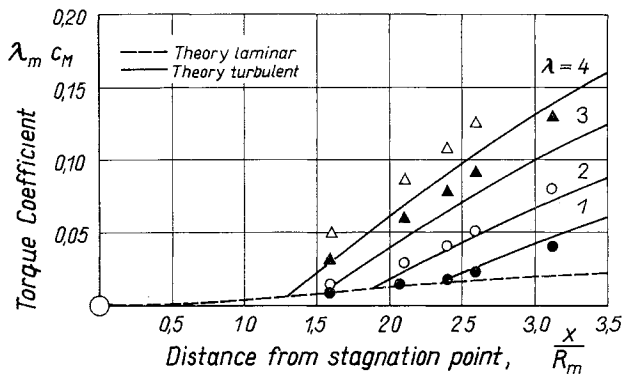


Fig 3 Torque coefficient as defined by Eq (5) on a spinning body of revolution; theory and experiment, $Re_m = 3 \times 10^5$, $\lambda = R_m \omega / U_m$

and by Luthander and Rydberg² for the rotating sphere. In more recent times, the general case of an arbitrary body of revolution has been investigated theoretically for laminar flow by Schlichting³ and for turbulent flow by Truckenbrodt⁴. Since there is not yet an experimental verification of the theoretical results, a thorough experimental investigation was carried out. In the course of this work, it seemed necessary to re-examine also the theory for turbulent flow. This note is an abstract of a recent publication⁵ reporting the results of these investigations.

For the experimental investigations, a cylindrical body with a blunt nose and a body of revolution with a slender rear part were chosen. The latter shape was chosen especially to investigate the effects of rotation on flow separa-

tion. The experiments were conducted in the following ranges of the two important parameters occurring in this problem, namely, the Reynolds number $Re_m = U_m R_m / \nu$ and the rotation parameter $\lambda_m = V_m / U_m$ (see Fig 1): Re_m from 3×10^5 to 9×10^5 , and λ_m from 0 to 4. The velocity profiles of the boundary layers on the spinning body of revolution are skewed due to the influence of rotation. An important result of the boundary-layer measurements is shown in Fig 1. The data points fit in well on the straight line given by

$$v/v_0 = 1 - (u/U) \quad (1)$$

for all values of the rotation parameter λ_m . This relation is used in the theoretical analysis.

The method of calculation is based on the momentum integral equations of the boundary layer in the meridional and circumferential direction using the two momentum loss thicknesses as defined by

$$\vartheta_x = \int_0^\delta \frac{u}{U} \left(1 - \frac{u}{U}\right) dz \quad (2)$$

$$\vartheta_{xy} = \int_0^\delta \frac{u}{U} \frac{v}{v_0} dz \quad (3)$$

For the solution of these equations, an assumption for the resultant skin friction at the wall τ_0 has to be introduced which depends on the rotation of the body. This is given by

$$\frac{\tau_0}{\rho U^2} = \frac{\alpha [1 + (v_0/U)^2]^{(n-2)/2}}{(U \vartheta_x / \nu)^n} \quad (4)$$

with the following numerical values: for laminar flow, $\alpha = 0.22$ and $n = 1$; for turbulent flow, $\alpha = 0.013$ and $n = 0.25$. In the case of no rotation, Eq (4) reduces to the well-known relation for the skin friction of a flat plate.

Using relation (4) the momentum integral equations have been solved by quadrature, and simple formulas have been obtained for the momentum thicknesses and the torque coefficient.

Some comparisons between the calculated and measured values of the meridional momentum loss thickness ϑ_x are given in Fig 2 for the cylindrical body with the blunt nose. On the whole, the agreement between theory and experiment is good. There is a strong dependence of the meridional momentum thickness ϑ_x on the rotation parameter λ_m in the turbulent regime. Furthermore, the point of transition from laminar to turbulent flow, which was determined with the aid of a hot wire anemometer, moves upstream with increasing rotation parameter. The influence of the Reynolds number is small in comparison with that of the rotation parameter. From the measurements on the body with a slender rear part, it has been concluded that the position of the point of separation is only slightly influenced by the rotation parameter.

Finally, a comparison of the calculated torque coefficient as defined by

$$c_M = \frac{M}{\frac{1}{2} \rho V_m^2 R_m^3} \quad (5)$$

with the measured values is given in Fig 3. The relation between c_M and ϑ_{xy} is given by

$$\lambda_m c_M = 4\pi \left[\frac{U}{U_m} \left(\frac{R}{R_m} \right)^3 \frac{\vartheta_{xy}}{R_m} \right]_{x_s} \quad (6)$$

Here, also, the agreement between theory and measurement is satisfactory.

References

- Wieselsberger, C., "Ueber den Luftwiderstand bei gleichzeitiger Rotation des Versuchskörpers," *Phys. Z.* 28, 84-88 (1927).

² Luthander, S and Rydberg, A "Experimentelle Untersuchungen über den Luftwiderstand bei einer um eine mit der Windrichtung parallelen Achse rotierenden Kugel," *Phys Z* **36**, 552-558 (1935).

³ Schlichting, H, "Die laminare Strömung um einen axial angeströmten rotierenden Drehkörper," *Ingr-Arch* **21**, 227-244 (1953)

⁴ Truckenbrodt, E, "Ein Quadraturverfahren zur Berechnung der Reibungsschicht an axial angeströmten rotierenden Drehkörpern" *Ingr-Arch* **22**, 21-35 (1954)

⁵ Parr, O, "Untersuchungen der dreidimensionalen Grenzschicht an rotierenden Drehkörpern bei axialer Anströmung," Ph D Thesis, Braunschweig (1962); also *Ingr-Arch* **32**, 393-413 (1963)

Earth Radius/Kilometer Conversion Factor for the Lunar Ephemeris

VICTOR C CLARKE JR *

Jet Propulsion Laboratory, Pasadena, Calif

I Introduction

IN precision simulations of lunar and interplanetary probe trajectories, the equations of motion contain terms that require a knowledge of the position of the moon at any time during flight. Furthermore, for calculation of the probe's position and velocity relative to the moon, both the position and velocity of the moon are required. Common practice is to obtain the position of the moon from the Lunar Ephemeris¹ and subsequently develop the velocity by numerical differentiation of the position.

A difficulty arises in that the lunar coordinates given in the Ephemeris use the earth radius as a unit of length, whereas, for practical reasons, a laboratory unit of length such as the kilometer is employed as the basic unit of measure in trajectory calculations. The problem is then one of determining a conversion (or scale) factor to convert the lunar coordinates from earth radii to kilometers.

At first impulse, one would choose the best available value of the earth equatorial radius, as expressed in kilometers, and use this as the conversion factor. However, to do so would be incorrect. Rather, the conversion factor must be computed from a relationship that is a function of the moon's mean motion and the gravitational constants of the earth and moon.

It is the purpose of this paper to develop this relationship and give a value for the earth radius/kilometer conversion factor for the Lunar Ephemeris.

II Analysis

De Sitter² defines the sine of the mean equatorial lunar parallax as

$$\sin \pi_{\epsilon} = b/a \quad (1)$$

where b is the equatorial radius of the earth and a is the "constant of the moon's variation orbit" defined in Brown's theory.^{3,4} The constant α is defined by the relation

$$n^2 \alpha^3 = GM_E + GM_M \quad (2)$$

where G is the universal gravitational constant, M_E and M_M are the masses of the earth and moon, and n is the moon's mean sidereal motion, which is taken as a fundamental in

variant, the value of which, as used by Brown, is $n = 0.2661699563 \times 10^{-5}$ rad/sec. Brown also gives a relation between a and α ; it is

$$a/\alpha = 0.999093141975298 \quad (3)$$

Thus, it is seen that, if $GM_E + GM_M$ and $\sin \pi_{\epsilon}$ are known, then b can be calculated. Brown gives

$$\sin \pi_{\epsilon} = 3422''.54 = 0.01659294212$$

Thus,

$$b/a = 0.01659294212$$

or

$$a = 60.2665876b \quad (4)$$

which establishes the relation between the mean lunar distance and earth radius as Brown sees it. From Eq (3),

$$\alpha = 1.000907681a \quad (5)$$

Then

$$\alpha = 60.32129044b \quad (6)$$

After substituting (6) into (2), we obtain

$$b = 0.0165778946[(GM_E + GM_M)/n^2]^{1/3} \quad (7)$$

or finally

$$b = 86.315745(GM_E + GM_M)^{1/3} \quad (8)$$

III Conclusion

The formula, Eq (8), is the relation mentioned earlier for computing the earth radius/kilometer conversion factor b , when GM_E and GM_M are given in kilometers cubed per seconds squared. This relation is analogous to Kepler's third law and must be maintained. If some other value of b is used, the well-determined mean motion of the moon is not preserved.

To calculate a value of b from Eq (8), let $GM_E = 398603.2$ km³/sec²⁵ and note that K_{ME} , "the coefficient of the indirect acceleration of the moon on the earth," has been well determined from the orbit of Mariner II,⁶ where

$$K_{ME} = GM_M/b^2 = 1.205116 \pm 0.000049 \times 10^{-4} \quad (9)$$

A cubic equation in GM_M can be formed by using Eq (8) and (9) to eliminate b and yield

$$GM_M = 4902.78 \pm 0.20 \text{ km}^3/\text{sec}^2$$

and thus give an earth-moon mass ratio of

$$\mu = 81.3015 \pm 0.0033$$

Subsequently, from Eq (9),

$$b = (GM_M/K_{ME})^{1/2} \quad (10)$$

or, finally, the numerical value of the earth radius/kilometer conversion factor is

$$b = 6378.3255 \text{ km}$$

Upon substituting this into Eq (4), we obtain the mean distance of the moon

$$a = 384399.9 \text{ km}$$

which compares favorably with Fischer's⁷ value of 384,400 km and the radar-determined value of 384,400 \pm 2 km.⁸

To conclude, it is important to realize that the value of earth radius b is not the same as the actual radius of the earth; it is merely the conversion factor and is used *only* for scaling the Lunar Ephemeris from earth radii to kilometers. The value of the actual radius of the earth R_E is taken to be $R_E = 6378.165$ km.⁵

Received August 22, 1963. This paper presents the results of one phase of research carried out at the Jet Propulsion Laboratory, California Institute of Technology, under Contract No. NAS 7-100, sponsored by NASA.

* Supervisor, Trajectories and Performances Group.